JOURNAL OF SOLID STATE CHEMISTRY 34, 97–106 (1980)

# X-Ray Study of the Ordering of the Alkali Ions in the Intercalation Compounds $Na_xTiS_2$ and $Li_xTiS_2$

TJIPKE HIBMA

*Brown Boveri Research Center, CH-5405 Baden-Dättwil, Switzerland*

Received May 8, 1979; in revised form August 6, 1979

The arrangement of the alkali ions in electrochemically intercalated $TiS_2$ crystals was studied by diffuse X-ray techniques. In $Na_xTiS_2$ a stage 3 phase was discovered in addition to the known stage 1 and 2 phases. Three types of three-dimensionally ordered superstructures were observed: a $(3^{1/2}\times 3^{1/2})$ superstructure for stage 2 and 3 phases, a $(2\times 2)$ and $(2\times 3^{1/2})$ superstructure for stage 1 and 2 phases. The appearance of these superstructures is consistent with a screened Coulomb interaction between the sodium ions. In the single-phase region above $x = 1/2$, diffuse rings show up in addition to the $(2\times 3^{1/2})$ superlattice. These rings are caused by local rearrangements of the ions to accommodate the excess sodium ions. The $(3^{1/2}\times 3^{1/2})$ and $(2\times 2)$ superstructures were also observed in $Li_xTiS_2$ crystals.

## I. Introduction

The alkali intercalation compounds of transition metal dichalcogenides are presently being intensively studied as possible electrode materials for electrochemical devices, such as batteries (*1*). In particular $Li_xTiS_2$ has received a lot of attention, because the intercalation process is highly reversible. This reversibility is associated with the fact that this material is single phase over the whole stoichiometry range, as has been deduced from the continuously changing cell parameters and emf as a function of $x$. This behavior is very different from what is observed in alkali metal intercalated graphite. In that case a number of stoichiometric phases called stages exist. In contrast to $Li_xTiS_2$ only a fraction of all available van der Waals layers are intercalated, and each filled layer has a fixed alkali ion content. For arbitrary compositions two stages are in equilibrium as is evident from the stepwise changing emf of the alkali metal/graphite intercalate cells (*4*). $Na_xTiS_2$ seems to take a position, which is intermediate between these two cases. Different stages are observed but each stage exists over a finite stoichiometry range.

The present study was undertaken to study the state of order of the alkali ion sublattice in $Li_xTiS_2$ and $Na_xTiS_2$ by diffuse X-ray scattering. This information is of crucial importance to understand the thermodynamic and transport properties of these materials.

Previous X-ray data (*2*) show that in $Na_xTiS_2$ at least three different phases can be observed, as far as a different stacking order of the constituent ions is concerned. Above $x \simeq 0.79$ the material is a stage 1 compound in which the $Na^+$ ions are in trigonal antiprismatic (distorted octahedral) positions. These sites form a triangular lattice. For $NaTiS_2$ all these sites are occupied. The $Li^+$ ions in $Li_xTiS_2$ are in the same type of sites. Ionic motion has to proceed via relatively small tetrahedral interstitial sites.



0022-4596/80/100097-10$02.00/0

Below $x = 0.68$ the sulfur layers below and above the alkali ions are right on top of each other, the $Na^+$ ions having a trigonal prismatic sulfur environment. These sites form a honeycomb lattice and are connected to each other through rectangles of sulfur ions. At lower $x$ values a stage 2 compound is stable, in which the sodium ions are most probably in the same type of sites. In the emf curve (*3*) also apparently three single-phase regions occur, but the phase boundaries do not agree with those of the X-ray results of Rouxel (*5*).

## II. Experimental

$TiS_2$ was prepared by heating the elements for several days at 600°C. A large excess of sulfur (~10%) was used and the material was cooled down very slowly in order to get near-stoichiometric $TiS_2$ (*3*). From this material $TiS_2$ crystals were grown by iodine vapor transport in a two-zone furnace, the temperature of the zones being 900 and 700°C. The stoichiometry of the crystals was checked by heating a weighted amount of $TiS_2$ in a stream of oxygen and calculating the titanium content from the weight difference. The crystals were stoichiometric within less than 1%. Well-developed crystals of 0.2 to 0.5 mg were intercalated electrochemically in thin-walled glass cells, 5 mm in cross section and 40 mm long. A solution of carefully dried NaI or $LiClO_4$ in propylene carbonate was used as the electrolyte and amalgamated sodium or lithium metal as the counterelectrode (*3*). The $TiS_2$ crystals were connected to the anode lead with a tiny bit of colloidal carbon. The intercalation was usually performed at a constant current of a few tenths of a microampere. Afterward at least 1 day was allowed to pass before the X-ray experiments were done.

The anode lead could be moved up and down, to draw the crystals out of the electrolyte solution, when making precession photographs. These pictures were used to determine the stacking sequence of the layers in the intercalated crystals. For the diffuse X-ray experiments the crystals had to be taken out of the cells, because the diffuse scattering and absorption of the glass tubes is too strong. To prevent rapid deterioration by moisture, the crystals were wrapped in Kapton tape in a dry box. The characteristic lines of the hydrated compounds appeared only after several days. The diffuse X-ray photographs were always carried out immediately after disassembly of the cells and afterward a precession photograph was taken to check whether the hydrated compounds were still absent. The diffuse X-ray pictures were taken with MoK$\alpha$ radiation, point-focused with a doubly bent LiF monochromator.

## III. Results

### 1. $Na_xTiS_2$

A considerable number of ordered structures appears to exist for different compositions of $Na_xTiS_2$. These different structures can be characterized by two factors: (a) the fraction of intercalated van der Waals layers and their stacking order, and (b) the ordering of the $Na^+$ ions within these layers.

(a) In Fig. 1 the average separation of successive titanium layers ($c_0$) is shown, as determined from precession photographs. In addition to the stage 1 and 2 phases already known (*2*), we have identified a stage 3 phase at low $x$ values. A rough estimate of $c_0$ for the high-order stages can be obtained, if one assumes that the thickness of an intercalated $TiS_2$ slab is the same for all stages (6.98 Å) and the thickness of an empty $TiS_2$ slab is equal to the $c$-parameter of $TiS_2$ (5.69 Å). The calculated values, 6.12 Å for the stage 3 phase and 6.33 Å for the stage 2 phase, agree well with the experimental values of 6.14 and 6.34 Å, respectively. Most probably also higher-order stages exist, but the most intense 00l lines predicted for the stages are very close to the corresponding lines of $TiS_2$.

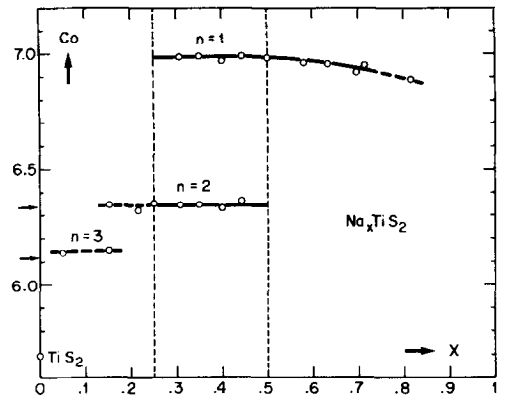


FIG. 1. The average separation of successive titanium layers in $Na_xTiS_2$. In addition to the known (Ref. (2)) stage 1 and 2 phases a stage 3 phase is observed at low $x$-values. Between $x=\frac{1}{4}$ and $x=\frac{1}{2}$ the stage 1 and 2 phases coexist. For $x>\frac{1}{2}$ the material is single phase.

Between $x=0.25$ and $x=0.50$ the stage 1 and 2 phases were found to coexist. This is a true two-phase region and does not result from insufficient chemical equilibrium of the crystals, because the lattice parameters of both phases are constant in this stoichiometry range.

Above $x=0.50$ the system is again single phase. A continuous change of the $c$-parameter was observed up to $x=0.81$, indicating that the $Na^+$ ions are still in trigonal prismatic sites up to this composition in our crystals, in contrast to the earlier powder diffraction data (5), indicating that the trigonal prismatic phase ends at $x=0.68$. This phase boundary probably depends on the way of preparation of the material. Haange *et al.* (6) recently prepared a metastable modification of $NaTiS_2$ in which the $Na^+$ ions are also in trigonal prismatic sites.

No reliable data could be collected above $x=0.81$, because the quality of the crystals becomes very poor at high sodium contents.

(b) Three different types of superstructures were observed associated with the ordering of the $Na^+$ ions in the intercalated layers (Table I). At low sodium contents ($x<0.25$) very weak superstructures of type

TABLE I

X-RAY DATA FOR $Na_xTiS_2$ CRYSTALS

| $x$ | Stage | Superstructure | $c_0$ (Å) |
|---|---|---|---|
| 0.05 | 3+$TiS_2$ | — | 6.14 |
| 0.07 | — | A+B | — |
| 0.139 | — | A+B | — |
| 0.150 | 3+$TiS_2$ | B | 6.15 |
| 0.152 | 2 | A | 6.342 |
| 0.200 | — | C+A | — |
| 0.216 | 2 | C+B | 6.32 |
| 0.250 | 2 | C | 6.348 |
| 0.286 | — | C | — |
| 0.300 | — | C | — |
| 0.302 | — | C | — |
| 0.308 | 1+2 | C | 6.343; 6.99 |
| 0.35 | 1+2 | C | 6.346; 6.99 |
| 0.372 | — | C | — |
| 0.385 | — | C | — |
| 0.399 | 1+2 | C | 6.328; 6.969 |
| 0.440 | — | C | — |
| 0.442 | 1+2 | C | 6.36; 6.99 |
| 0.50 | 1 | C | 6.977 |
| 0.55 | 1 | C+diff. rings | — |
| 0.581 | 1 | — | 6.96 |
| 0.652 | — | A+diff. rings | — |
| 0.696 | 1 | A+diff. rings | 6.917 |
| 0.71 | — | A | — |
| 0.712 | 1 | — | 6.95 |
| 0.762 | — | A | — |
| 0.815 | 1 | — | 6.89 |

A or B (Fig. 2) or both were observed, corresponding to a quadruple or triple unit cell, respectively. In this stoichiometry range it was difficult to get homogeneously intercalated crystals. For $x<0.15$ usually some unchanged $TiS_2$ was present. This circumstance does not allow one to assign definite stoichiometries or stoichiometry ranges to the observed superstructures. However, it is likely that they correspond to the equidistant $Na^+$ superlattice with $a_A=2a$ and $a_B=3^{1/2}a$ with one $Na^+$ ion per unit cell per layer, suggesting that two ordered stage 2 phases with $x=\frac{1}{6}$ and $x=\frac{1}{8}$ and at least one stage 3 phase with $x=\frac{1}{9}$ exist.

For $0.25<x<0.50$ exclusively the rather complicated pattern C is found (Fig. 2). As an example the pattern for $x=0.44$ is shown in

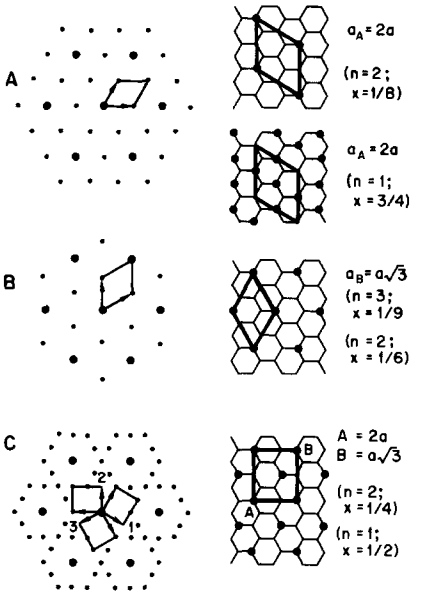


FIG. 2. The observed superstructure patterns and the corresponding unit cells in $Na_xTiS_2$. Pattern C consists of a superposition of the $(2\times3^{1/2})$ superstructure of three rotational twins. Note that the patterns are projections of the superlattice spots onto the basal plane.

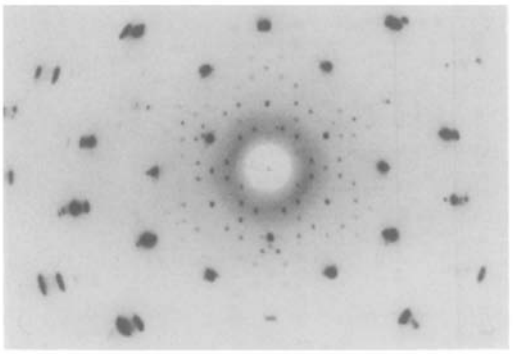

FIG. 3. Oscillation (16°) picture of $Na_{0.44}TiS_2$, showing the superstructure pattern C of Fig. 2. The satellites of the Bragg spots of the rhombohedral substructure are probably associated with the mismatch between the stage 1 and stage 2 phases.

Fig. 3. As will be shown in the next section the corresponding arrangement of $Na^+$ ions is one in which one out of four trigonal prismatic sites is occupied by a $Na^+$ ion. The stage 1 phase therefore must correspond to $x = \frac{1}{2}$ in agreement with the upper boundary of the two-phase region (Fig. 1). The intensity of the superstructure pattern decreases with decreasing $x$, but no other changes occur. The arrangement of the $Na^+$ ions in the stage 2 phase is likely to be the same as that for the stage 1 phase and its composition is $x = \frac{1}{4}$, again consistent with the lower boundary of the two-phase region.

For $x$ slightly above 0.50 the superstructure C is still present but in addition weak diffuse rings appear (Fig. 4). As is shown in the next section these rings are caused by small disordered regions, which are induced by introducing excess $Na^+$ ions in the $Na_{0.50}TiS_2$ structure. For still larger values of $x$ both the superstructures of $Na_{0.50}TiS_2$ and the diffuse rings disappear and a relatively weak superstructure of type A appears again. Because the unit cell of this superstructure is four times as large as the cell of the $TiS_2$ substructure, it is likely that the ions are arranged as is shown in Fig. 2. This arrangement corresponds to a composition of $x = \frac{3}{4}$. No pictures were taken for $x \geq 0.81$, because the quality of the crystals decreases rapidly at very high sodium contents.

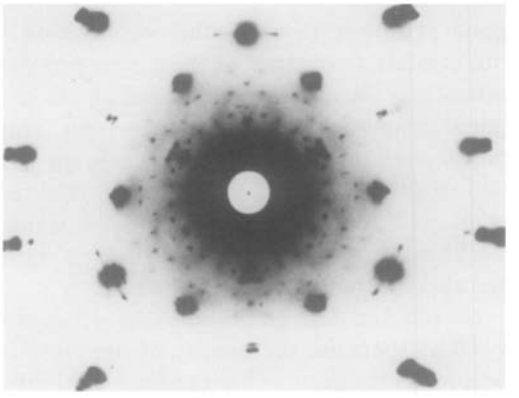

FIG. 4. Oscillation (16°) picture of $Na_{0.55}TiS_2$. The black region in the center is caused by the protecting Kapton foil. Apart from the superstructure pattern C, faint diffuse rings appear, the diameter of which decreases with increasing $x$.

*2. $Li_xTiS_2$*

In contrast to the sodium intercalates, no homogeneously intercalated crystals could be obtained even for high lithium contents. Always a relatively large part of the crystals consisted of unchanged $TiS_2$. Although the relative amount decreased in time (as was deduced from the decrease of the $c$-parameters of the intercalated part) even after several weeks no equilibrium was established. For all nominal $x$-values studied the $c$-parameter eventually dropped considerably below the values given in Ref. (*7*). The reflections arising from the intercalated part of the crystals were sharp. The intercalated part of the crystals therefore is single phase, indicating that within the layers equilibrium is established relatively fast.

Superstructures of type A or B or both were observed. Because Li has a very small structure factor compared to Ti and S, the intensities of the superstructure reflections are most probably caused by small displacements of the sulfur ions induced by the arrangements of the $Li^+$ ions. For a nominal stoichiometry of $x = 0.19$ the type A superstructure could be analyzed in more detail. The supercell appears to be doubled in the $c$-direction. The stoichiometry of the ordered structure related to this superstructure is most probably $\frac{1}{4}$. The $Li^+$ ions then are arranged on a triangular lattice, with a lattice parameter, which is twice as large as the $TiS_2$ sublattice parameter $a$. Successive $Li^+$ layers are shifted over a distance of $a$ in the 100 or equivalent direction.

## IV. Analysis of the Diffraction Patterns

*1. $Na_xTiS_2$ ($0.25 < x < 0.50$)*

At first sight the superstructure in this stoichiometry range (Fig. 2C) appears to have a unit cell 16 times as large as the unit cell of $TiS_2$ in the hexagonal plane. However, the absence of a large number of reflections suggests that the pattern is a superposition of three rotationally equivalent lattices having a rectangular unit cell. This unit cell corresponds to the orthohexagonal cell of the $TiS_2$ structure doubled along the short axis:

$$\mathbf{A} = 2\mathbf{a},$$

$$\mathbf{B} = \mathbf{a} + 2\mathbf{b}.$$

Reflections are systematically absent for $3H + 2K = 6n + 3$. Therefore there is at least one pair of ions per unit cell in each plane related by a translation:

$$\mathbf{R} = \mathbf{A}/2 + \mathbf{B}/3.$$

Because of the size of the $Na^+$ ions only one such pair can be accommodated in a unit cell. The arrangement of the ions therefore must be as depicted in Fig. 2C.

To study the superstructure in the $c$-direction a series of Polaroid pictures were taken from a static crystal of composition $x = 0.50$, rotating the crystal over 1° each time, around an axis perpendicular to the hexagonal axis. From these pictures the corresponding part of the reciprocal lattice was constructed.

The smallest possible unit cell is triclinic. However, in order to show the relation between the superstructure and the $TiS_2$ substructure, we will analyze it in orthorhombic coordinates. For $H = 2n$ the spacing between successive spots along $c$ for a given $H$ and $K$ value is $c_0^*$ (where $c_0$ is the separation of two successive $Na^+$ layers). Although the positions of the reflections for $H = 2n + 1$ cannot be determined accurately from the diffuse X-ray pictures because they overlap, it is clear from oscillation pictures that there are twice as many reflections. These observations are in agreement with the conditions for possible reflections:

$$\tfrac{1}{4}H \pm \tfrac{1}{6}K + \tfrac{1}{12}L = n.$$

These conditions correspond to a shift of either $\frac{1}{4}\mathbf{A} + \frac{1}{6}\mathbf{B}$ or $\frac{1}{4}\mathbf{A} - \frac{1}{6}\mathbf{B}$ between successive $Na^+$ layers. For the orthorhombic unit cell therefore we have $C = 12\ c_0$. The two shifts

above are equivalent and cause an additional twin, related by the mirror planes of the substructure.

The superstructure of $Na_{0.30}TiS_2$ was studied in the same way. For this predominantly stage 2 compound the spacing between the $H = 2n$ reflections should be $\frac{1}{2}c_0^*$; the only difference with respect to the stage 1 case, however, was that the structure was much more diffuse. This suggests that the stacking of the $Na^+$ layers is not very well defined in the stage 2 phase.

### 2. $Na_xTiS_2$ ($x > 0.50$)

In this stoichiometry region all our data are in accordance with a single-phase behavior. The average lattice is still the same as is found for the $Na_{0.5}TiS_2$ structure but some disorder must be present because in addition diffuse ring-like structures are observed. As we will discuss in more detail in the next section, the interaction between the $Na^+$ ions is most probably a screened Coulomb interaction, i.e., a relatively rapidly decreasing function of the separation between the ions. We will use this result to construct the disordered arrangement of the $Na^+$ ions, and show that the diffuse X-ray intensity distribution calculated for this arrangement qualitatively agrees with that observed.

To accommodate an excess $Na^+$ ion in the $Na_{0.50}TiS_2$ structure at least one ion has to be displaced to a neighboring interstitial site because two nearest-neighbor (nn) sites of the honeycomb lattice are too close to each other to be occupied simultaneously. In this way a defect region is created consisting of a pair of ions and a vacancy. There are five nearest-neighbor bonds of length $a$ in such a defect region (Fig. 5a). More complicated defect regions can be constructed by putting more excess $Na^+$ ions in. If we now assume that the main part of the excess lattice energy arises from the nearest-neighbor interactions, these disordered domains should satisfy the condition that the number of nn

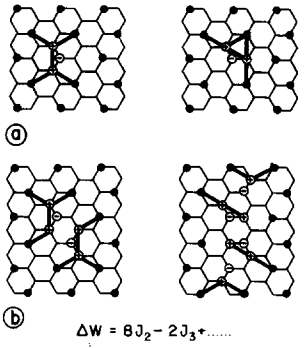


FIG. 5. (a) To accommodate an extra ion in the $Na_{0.5}TiS_2$ structure (Fig. 2C), one $Na^+$ ion has to be displaced to a neighboring site. This can be done in two different ways. (b) By combining two such defects the number of nn bonds per excess ion can be reduced from 5 to 4.

bonds is a minimum. By inspection it was found that a minimum of 4 nn bonds is obtained if two of the above-mentioned defect regions are combined as shown in Fig. 5b. In one of the possibilities the number of nnn bonds can be reduced by displacing two additional ions. More complicated disordered regions, having the same number of nn bonds per $Na^+$ ion, are also possible, but they are much less probable, because more than two excess $Na^+$ ions are involved and we will assume that the disorder for $x > 0.5$ may be described as a statistical distribution of the defect regions shown in Fig. 5b.

If the number of defect regions is sufficiently small, the diffuse X-ray scattering intensity is given by

$$I_D = \sum_i n_i |F_0 - F_i|^2, \qquad (1)$$

where $n_i$ is the number of defect regions of type $i$, $F_i$ their structure factor, and $F_0$ the corresponding structure factor of the undisturbed structure.

Using this expression, the diffuse intensity was calculated for a statistical distribution of the defect regions shown in Fig. 5b and all symmetry-equivalent regions. The result is shown in Fig. 6. The qualitative similarity between the calculated and the observed distribution is remarkable. Even the

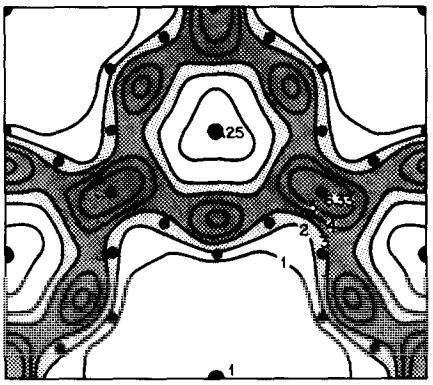


FIG. 6. Calculated diffuse intensity for a statistical distribution of defect regions of the type shown in Fig. 5b. The numbers on the equi-intensity lines are the intensity values for a scattering factor of 1. Also drawn are the sublattice and superlattice diffraction spots.

diameters of the diffuse rings are very close. For a quantitative comparison it would be necessary to include more complicated disordered regions in the calculation. These probably are responsible for the decrease of the diameter of the rings with increasing $x$. The inhomogeneity, the poor quality of the crystals, and the strong background due to the Kapton foil, used to prevent deterioration of the crystals by moisture, do not allow such a quantitative analysis.

In the above model it can also be understood why the system is single phase in this stoichiometry region and not a mixture of the $Na_{0.5}TiS_2$ phase and the ordered phases for $x = \frac{2}{3}$ or $x = \frac{3}{4}$ which can be imagined. The minimum number of nn bonds per excess $Na^+$ ion is obtained for the hexagonal superstructures with $a_B = 3^{1/2}a$ and $a_A = 2a$, respectively, and is equal to 12 in both cases, much larger than the number obtained for the disordered structure described above, which is 4.

## V. Comparison with Other Data

### 1. $Na_xTis_2$

Although our study confirms the results of Ref. (*2*) in the sense that a number of different stages exist in $Na_xTiS_2$, their phase limits (*5*) are very different from ours. Whereas we find that the stage 1 and 2 phases coexist between $x = 0.25$ and $x = 0.50$, Rouxel and co-workers find a much smaller two-phase region between $x = 0.33$ and 0.38. In Ref. (*2*) polycrystalline $TiS_2$ was treated with Na dissolved in liquid $NH_3$, followed by heating at 250°C in order to remove $NH_3$. This different technique of preparation of the samples somehow may be responsible for the observed differences (*1*). It should be noted, however, that the phase limits from our study are not only based on phenomenological data, but also on the compositions consistent with the observed sodium superstructures.

The agreement between our data and the emf data of Winn and Steele (*3*), who also used electrochemically intercalated crystals, is somewhat better (see Fig. 7). Abrupt changes of slope in the emf vs $x$ curve of a $Na_xTi_yS_2/Na$ cell are observed at $x = 0.46$ and 0.80 for $y = 1.002$, at $x = 0.46$ and 0.70 for $y = 1.01$, and at $x = 0.52$ and 0.77 for $y = 1.02$, values which are close to the compositions $x = 0.50$ and 0.75 corresponding to the ordered sodium arrangements we find for the stage 1 phase. Below $x \simeq 0.50$ the emf curves are rather flat, consistent with a two-phase region. At $x = 0.25$ the stage 2

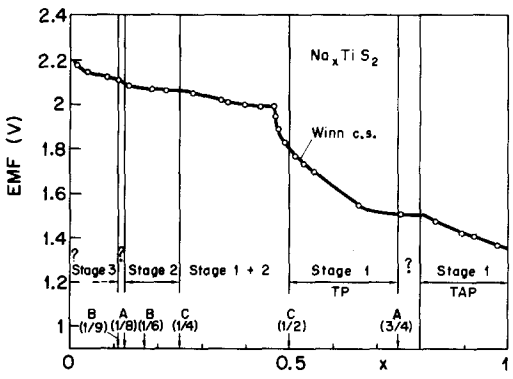


FIG. 7. Comparison between the phases found by X rays and the emf of $Na_xTiS_2$ with respect to sodium (Ref. (*3*)).

phase ends. In some of the emf curves presented in Ref. (*3*) a break is indicated at this $x$-value although the authors did not recognize it as such. Below $x = 0.25$ the situation is complicated by the occurrence of several superstructures and stages. The inhomogeneity of the crystals in this range does not allow one to assign stoichiometry ranges to the stage 2 and stage 3 compounds.

*2. $Li_xTiS_2$*

Recently a very careful measurement of the derivative of the composition with respect to the emf was carried out for the $Li/TiS_2$ electrochemical cell (*9*). The peaks at a number of definite fractional compositions were interpreted by assuming that ordered superlattices exist for the Li ions. Our results confirm these findings. The A-type superstructure with a fourfold unit cell in the hexagonal plane and a doubled $c$-parameter is very probably connected with $x = \frac{1}{4}$, in agreement with the most prominent peak in the $\Delta x/\Delta V$ curve. The B-type superstructure with a threefold unit cell, which was observed too in some instances, might correspond to the structure at about $x = \frac{1}{3}$.

## VI. Discussion

The most striking difference between the sodium and potassium intercalates of $TiS_2$ is that in $Li_xTiS_2$ all van der Waals layers are intercalated even for small $x$-values, whereas in $Na_xTiS_2$ a number of different stages occur. Offhand the reason for this different behavior is not at all clear. In the simplest picture of these compounds, the valence electron has been completely transferred to the conduction band of the $TiS_2$ slabs. The very small Knight shift observed for both $Li_xTiS_2$ (*7*) and $Na_xTiS_2$ (*10*) is consistent with this picture. Whether different stages will occur or not depends on the difference in formation energy of a (hypothetical) stage 1 and a higher-stage compound, having the same overall alkali content. This energy difference can be split up into the following contributions (*11*):

(a) The difference in energy required to separate the $TiS_2$ layers.

(b) The difference in Fermi energy (the distribution of the valence electrons over the $TiS_2$ layers may be inhomogeneous for higher stages (*12*)).

(c) The difference in interaction energy between the alkali ions within a layer.

(d) The difference in bonding energy between the alkali ion layers and the rest of the lattice.

The last two terms are probably the most important ones. In the case of complete charge transfer only the first and the last term depend somewhat on the nature of the cation through its size, but it is unlikely that the resulting small differences in binding energy are sufficient to explain the different behavior of the Li and Na intercalation compounds. In a recent calculation of the electron density distribution in the graphite intercalation compound $Li_6C$ (*13*), it was shown that relatively strong chemical binding exists between the Li and C layers, in spite of the fact that the Li entity is completely ionized in the sense that the valence electron is transferred to partially filled bands. The valence electron density between the layers of intercalated ions and the neighboring host layers of course depends very strongly on the nature of the cation. Even if their contribution to the total binding energy of the alkali ions is small, similar deviations from ideal charge transfer in the alkali intercalates of $TiS_2$ could account for the fact that different stages are observed in $Na_xTiS_2$ but not in $Li_xTiS_2$.

As was pointed out by Kaburagi and Kanamori (*14*) the occurrence or absence of ordered structures on a given lattice can give information about the nature of the interparticle interactions. Using the phase diagrams the above authors derive for a two-dimensional triangular lattice, Thompson (*9*)

showed that the ordered structures appearing in $Li_xTiS_2$ are consistent with a Coulomb type of interaction.

In $Na_xTiS_2$ a qualitative idea about the range and type if interactions between the $Na^+$ ions within a layer can be obtained by comparing the lattice energy of the observed superstructures of type A, B, and C (Fig. 2) with the lattice energy of other possible superstructures, which are not observed, but could be imagined, i.e., the structures A', B', and C' of Fig. 8.

The lattice energy can be expressed as

$$W = \sum_i n_i J_i,$$

where $J_i$ is the interaction between $i$th neighbors. If we cut off this sum after the sixth neighbor on a honeycomb lattice and assume that the lattice energy of the observed superstructures is smaller than the lattice energy of the corresponding hypothetical superlattices, we find that

$$J_3 > 2J_4 > 4J_5 > 8J_6.$$

The interaction therefore is a strongly decreasing function of the interionic distance. In fact the decrease is much stronger than a simple Coulomb law would predict. The Coulomb interaction therefore must be screened considerably by the conduction electrons of the $TiS_2$ slabs. This result justifies the neglect of other than nearest-neighbor interactions in the calculation of the diffuse X-ray scattering of the last section.

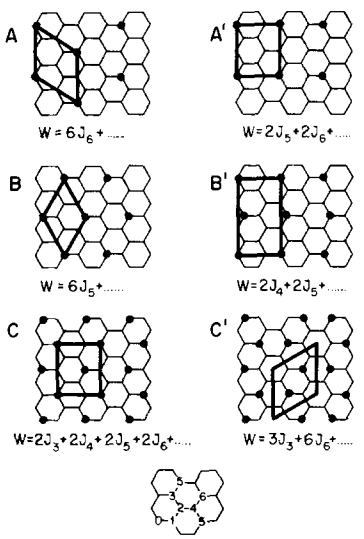


FIG. 8. A comparison between lattice energies of the observed structures A, B, and C and those of three hypothetical structures for the same composition (A', B', and C') leads to the inequality for the interaction potentials $J_i$ for $i$th neighbors: $J_3 > 2J_4 > 4J_5 > 8J_6$, if interactions up to sixth neighbors are taken into account. This fast decrease of the interaction with separation between ions indicates a considerable screening by the conduction electrons.

## VII. Summary

An important result of this study is that the superstructures observed in both $Li_xTiS_2$ and $Na_xTiS_2$ consist of sharp Bragg spots, showing that a well-defined three-dimensional average superlattice exists. Thus long-range correlations among the alkali ions must exist, not only within the alkali layers but also between different alkali layers. On the other hand the alkali ion sublattice must be disordered to some extent for arbitrary compositions, because emf measurements show that within each stage a finite stoichiometry range exists where the material is single phase. For $Na_{0.55}TiS_2$ the nature of this disorder was studied in some detail. The tendency to order as well as possible reflects the relatively low ionic conductivity for these materials (*3*) at room temperature. At higher temperatures a transition to a disordered state, in which only short-range order persists, might well occur. Such transitions have been observed in some copper and silver intercalation compounds of transition metal chalcogenides (*15*).

Finally, it should be realized that considerable uncertainties concerning details of the phase diagrams of $Na_xTiS_2$ and $Li_xTiS_2$ still remain. Many of the discrepancies between different studies are

undoubtedly associated with differences in preparing the materials. It therefore seems desirable to find methods to prepare homogeneously intercalated crystals of well-defined stoichiometry.

## References


1. M. S. WHITTINGHAM, *Progr. Solid State Chem.* **12**, 41 (1978); J. ROUXEL, *Rev. Inorg. Chem.*, in press.
2. J. ROUXEL, M. DANOT, AND J. BICHON, *Bull. Soc. Chim. Fr.*, 3930 (1971); J. BICHON, M. DANOT, AND J. ROUXEL, *C.R. Acad. Sci.* **276**, 1283 (1973); A. LEBLANC-SOREAU, M. DANOT, L. TRICHET, AND J. ROUXEL, *Mater. Res. Bull.* **9**, 191 (1974).
3. D. A. WINN AND B. C. H. STEELE, *Mater. Res. Bull.* **11**, 551 (1976); D. A. WINN, J. M. SHEMILT, AND B. C. H. STEELE, *Mater. Res. Bull.* **11**, 559 (1976).
4. S. ARONSON, F. J. BALZANO, AND D. BELLAFIORE, *J. Chem. Phys.* **49**, 434 (1968).
5. J. ROUXEL, *in* "Physics and Chemistry of Compounds with Layered Structures" (F. Levy, Ed.), Vol. VI, Reidel, Dordrecht (1979).
6. R. J. HAANGE, A. J. A. BOS-ALBERINK, AND G. A. WIEGERS, *Ann. Chim. Sci. Mater.* **3**, 201 (1978).
7. B. G. SILBERNAGEL AND M. S. WHITTINGHAM, *J. Chem. Phys.* **64**, 3670 (1976).
8. A. NAGELBERG AND V. L. WORRELL, *J. Solid State Chem.* **29**, 345 (1979).
9. A. H. THOMPSON, *Phys. Rev. Lett.* **40**, 1511 (1978).
10. B. G. SILBERNAGEL AND M. S. WHITTINGHAM, *Mater. Res. Bull.* **11**, 29 (1976).
11. F. J. SALZANO AND S. ARONSON, *J. Chem. Phys.* **44**, 4320 (1966).
12. L. PIETRONERO, S. STRÄSSLER, AND H. R. ZELLER, *Phys. Rev. Lett.* **41**, 763 (1978).
13. L. A. GIRIFALCO AND N. A. W. HOLZWARTH, *Mater. Sci. Eng.* **31**, 201 (1977).
14. M. KABURAGI AND J. KANAMORI, *J. Phys. Soc. Japan* **44**, 718 (1978).
15. F. W. BOSWELL, A. PRODAN, AND J. M. CORBETT, *Phys. Status Solidi A* **35**, 591 (1967); F. M. R. ENGELSMAN, G. A. WIEGERS, AND F. JELLINEK, *J. Solid State Chem.* **6**, 574 (1973).